Reports

BioTechniques

A compact and simple method of achieving differential transgene expression by exploiting translational readthrough

James E Sillibourne[1], Giulia Agliardi[1,2], Matteo Righi[1], Katerina Smetanova[1], Grant Rowley[1,3], Simon Speller[1], Abigail Dolor[1], Katarina Lamb[1], Christopher Allen[1], Rajeev Karattil[1], Farhaan Parekh[1], Frederick Arce Vargas[1], Simon Thomas[1], Shaun Cordoba[1] & Martin Pule*[,1,2]

*[1]Autolus Therapeutics plc, Mediaworks, 191 Wood Lane, London, W12 7FP, UK; [2]Department of Haematology, University College London Cancer Institute, Paul O'Gorman Building, London, WC1E 6DD, UK; [3]Department of Biochemistry, Imperial College London, South Kensington Campus, London, SW7 2AZ, UK; *Author for correspondence: m.pule@autolus.com*

BioTechniques 72: 00–00 (April 2022) 10.2144/btn-2021-0079

First draft submitted: 18 August 2021; Accepted for publication: 10 February 2022; Published online: 1 March 2022

ABSTRACT

The development of multicistronic vectors enabling differential transgene expression is a goal of gene therapy and poses a significant engineering challenge. Current approaches rely on the insertion of long regulatory sequences that occupy valuable space in vectors, which have a finite and limited packaging capacity. Here we describe a simple method of achieving differential transgene expression by inserting stop codons and translational readthrough motifs (TRMs) to suppress stop codon termination. TRMs reduced downstream transgene expression ~sixfold to ~140-fold, depending on the combination of stop codon and TRM used. We show that a TRM can facilitate the controlled secretion of the highly potent cytokine IL-12 at therapeutically beneficial levels in an aggressive immunocompetent mouse melanoma model to prevent tumor growth. Given their compact size (6 bp) and ease of introduction, we envisage that TRMs will be widely adopted in recombinant DNA engineering to facilitate differential transgene expression.

METHOD SUMMARY

We describe a simple method enabling two or more gene products to be synthesized in a cell at different levels to aid in the development of new therapeutics.

GRAPHICAL ABSTRACT

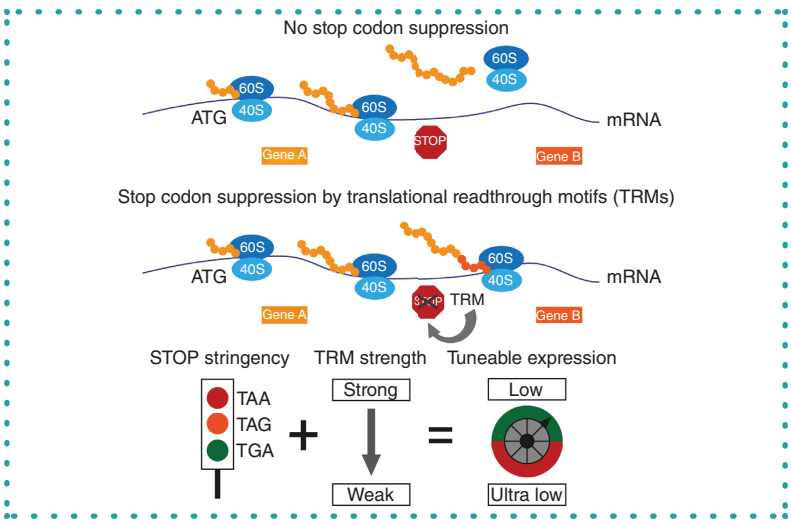

KEYWORDS:

cancer ● chimeric antigen receptor ● differential transgene expression ● immunotherapy ● packaging limit ● T cell ● translational readthrough motif ● ultra-low expression

Differential transgene expression can be vital to the success of some gene therapies, and developing methods to facilitate this is of paramount importance. In the case of chimeric antigen receptor (CAR) T-cell therapy (CAR-T), differential transgene expression can increase its efficacy through the regulated expression of stimulatory molecules. CARs endow T cells with the ability to target antigen-bearing cells in an MHC-independent manner [1,2] and are being used to target tumor and autoreactive immune cells. While CAR-T has proven successful for the treatment of blood malignancies, with three anti-CD19 CARs being granted US FDA approval for the treatment of B-cell acute lymphoblastic leukemia [3,4] and relapsed/refractory diffuse large B-cell lymphoma [5], there has been limited success in clinical trials treating solid tumors. Many factors are responsible for the limitations of CAR-T in treating solid tumors, but it has become clear that additional stimulatory or blocking molecules are required to enhance the function of CAR T cells. Recent approaches include the expression of cytokines, such as IL-12, to activate tumor-infiltrating T cells to promote the clearance of tumor cells [6]. However, such approaches must be adopted with considerable caution because cytokines are highly potent and their activation of the immune system can cause severe toxicity [7].

Researchers have sought to overcome toxicity problems by downregulating the expression of stimulatory molecules. Several approaches have been tested, including the use of attenuated internal ribosome entry sites (IRESs) [8], inducible promoter systems [6] and riboswitches [9]. While these approaches offer the ability to downregulate transgene expression, their main disadvantage is that they are typically long sequences (>100 bp) and represent a significant packaging burden when used in viral vectors. This is particularly pertinent when adeno-associated virus (AAV) is used as a vector, because it has a packaging limit of approximately 5 kb [10] and inclusion of the above-mentioned regulatory elements would take up valuable space. With the increasing use of AAVs in gene therapies, including as homology-directed repair templates to facilitate the insertion of transgenes during genome editing (such as CAR-encoding sequences to the T-cell receptor α-chain locus of primary T cells [11,12]), the ability to differentially express a second transgene from the same cassette could be extremely beneficial.

To circumvent this problem, we have investigated the insertion of stop codons (TGA, TAG or TAA) and short translational readthrough motifs (TRMs) [13–15] to facilitate differential transgene expression in multicistronic retroviral genomes. When a ribosome encounters a stop codon (TGA, TAG or TAA), translation is usually terminated by release factors [16,17], but occasionally stop codon suppression occurs due to competition between release factors and near-cognate transfer RNAs, resulting in the insertion of an amino acid and continued translation [13,15]. Readthrough can occur during the translation of endogenous and viral mRNAs. Several human mRNAs have been reported to undergo translational readthrough [13,18], generating proteins with extended C-termini that often exhibit altered function or subcellular localization. An example of this is LDHB, which is subject to functional translational readthrough, leading to the synthesis of a protein with an extended C-terminus encoding a peroxisome-targeting signal type 1 [19]. The inclusion of this peroxisome-targeting signal in LDHB extended redirects it from the cytoplasm to peroxisomes, where it is speculated to participate in the conversion of lactate to pyruvate and the degradation of long-chain fatty acids [19]. Translational readthrough occurs during translation of Moloney murine leukemia virus (MoMLV) *gag-pol*, with suppression of the TAG stop codon located 3′ of *gag* resulting in the insertion of a glutamine [20] and translation of the downstream *pol* gene by approximately 10% of ribosomes [20,21].

Translational readthrough is promoted by *cis*-acting elements located 5′ and 3′ of the stop codon. The four nucleotides immediately 3′ of the stop codon are important in promoting translational readthrough, and data suggest that a single cytidine 3′ of the stop codon is instrumental in mediating stop codon suppression [22]. Distal *cis*-acting elements can also influence translational readthrough, as in the case of MoMLV *gag-pol* where an RNA pseudoknot promotes translational readthrough of the TAG stop codon located 3′ of *gag*, resulting in the translation of *pol* [21,23].

Here we demonstrate that insertion of stop codons and short TRMs of no more than six bases enables differential transgene expression, with ∼sixfold to ∼140-fold reductions in transgene expression downstream of the TRMs. Differential transgene expression facilitated by TRMs is broadly applicable to recombinant DNA engineering technology in viral, bacterial, yeast and mammalian systems.

Materials & methods

Constructs

All open reading frames were cloned into the MoMLV-based retroviral genome construct SFG [24]. Cloning was carried out using Q5 DNA polymerase (NEB UK Ltd., Watford, UK; M0491L) and oligonucleotides (IDT, Leuven, Belgium) to amplify the coding sequences and to incorporate stop codons, TRMs and self-cleaving peptide sequences derived from *Thosea asigna* virus 2A (T2A), equine rhinitis A virus polyprotein or porcine teschovirus-1 2A. Type IIS restriction enzyme sites were incorporated into the oligonucleotides, and the resulting PCR products digested with *Esp*3I or *Bsa*I-HF v2 (NEB; R0734L and R3733L, respectively), purified and ligated together using T4 DNA ligase (Roche; 10799009001 – distributed by Merck Life Science UK Ltd., Watford, UK). Secreted embryonic alkaline phosphatase (SEAP) constructs were generated by cloning its coding sequence 3′ to the sort-select marker RQR8 [25]. Human CD22/CD19 chimera constructs were generated by fusing residues 1 to 20 of the murine immunoglobulin κ-chain V-III (representing signal peptide sequence) to residues 20 to 687 of human CD22 and residues 294 to 332 of human CD19. The CD22/CD19 chimeric sequence was cloned 3′ to the RQR8, TRM and self-cleaving peptide sequences. Enhanced blue fluorescent 2 protein (eBFP2) and mClover fluorescent protein constructs were generated by cloning the sequences 3′ of the marker gene *HA8*, consisting of residues 98–106 of human influenza hemagglutinin

(HA) fused to residues 141–222 of human CD8α. The IRES from encephalomyocarditis virus isolate JZ1202 (sequence ID: KF836387) was cloned from bases 148 to 734. IRES mutant 1 contained an additional A at 661 in the A6 bifurcation loop [26], and IRES mutant 2 possessed mutations at 150 C>G, 162 C>deleted, 337 A>G, 456 G>A, 462 A>G, 630 G>A and 661 insertion A [8,27]. CARs recognizing EGFRvIII [28] and the ganglioside GD2 [29] with murine CD8 spacer and transmembrane domains and murine CD28 and CD3ζ intracellular domains were cloned into SFG with an upstream Thy1.1 (murine CD90 marker). Murine flexi-IL-12, consisting of the p35 and p40 subunits of IL-12 fused together via an $S(GGGGS)_3$ flexible linker, was cloned downstream of the CARs. Human flexi-IL-12, consisting of the p35 and p40 subunits of IL-12 fused together via an $S(GGGGS)_3$, was cloned into SFG. Murine GD2 and GD3 synthase were cloned into SFG with an intervening equine rhinitis A virus polyprotein self-cleaving peptide sequence.

Cell culture & transfections

Cell lines were cultured at 37°C in a humidified incubator with 5% CO_2. HeLa (ATCC, VA, USA; CCL-2), 293T (ATCC; CRL-11268), Phoenix-ECO (ATCC; CRL-3214) and SCLC-21H (DSMZ, Braunschweig, Germany; ACC 372) cells were cultured in Iscove's modified Dulbecco's medium (IMDM; Sigma; I3390-500ML) and SupT1 cells (ECACC; 95013123 – distributed by Merck Life Science UK Ltd., Watford, UK) in RPMI-1640 (Sigma; R5886-500ML – distributed by Merck Life Science UK Ltd., Watford, UK). All media were supplemented with 10% fetal bovine serum (BioSera; FB-1001/500 – distributed by Labtech International UK Ltd., Heathfield, UK) and 2 mM GlutaMAX (Gibco; 35050061 – distributed by Fisher Scientific UK Ltd., Loughborough, UK). For 293T transfections, cells were plated in six-well plates (3×10^5 cells/well) and were transfected 24 h later with 2 μg of plasmid DNA using GeneJuice transfection reagent (Merck Millipore; 70967-3 – distributed by Merck Life Science UK Ltd., Watford, UK) at a 3:1 ratio (transfection reagent to DNA) according to the manufacturer's instructions. The cells were cultured for 48 h prior to carrying out enzyme-based or flow cytometric analyses.

Production of retroviral supernatants & cell transduction

Retroviral supernatants were produced by plating 2.4×10^6 293T cells in 10-cm plates and transfecting 24 h later with 4.7 μg of γ-retroviral genome plasmid, 3.1 μg RD114 (RDF glycoprotein) and 4.7 μg of PeqPam-env (MoMLV *gag-pol*), using GeneJuice transfection reagent at a ratio of 3:1 transfection reagent to DNA. For the transduction of murine splenocytes, supernatants were produced by transfecting Phoenix Eco cells with 4.68 μg DNA of γ-retroviral genome plasmid and 2.6 μg of pCL-ECO, encoding gagpol and Eco envelope glycoprotein, using GeneJuice transfection reagent as described above. Cell culture media, containing viral particles, were collected at 48 and 72 h after transfection, with the harvested media being replaced with fresh medium at 48 h. Retroviral transductions were carried out by plating 0.3×10^6 cells/well in 24-well non-tissue culture plates (Corning Falcon; 351147 – distributed by Fisher Scientific UK Ltd., Loughborough, UK), previously coated with retronectin (Takara Bio Ltd., London, UK; T100B) for 16–24 h at 4°C, adding the appropriate volume of retroviral supernatant and centrifuging at 1000 × *g* for 20 min at ambient temperature. The cells were returned to the incubator for 72 h prior to analysis.

SEAP assays

Supernatant was collected from cells 48 h after transfection and 20 μl analyzed for SEAP activity by adding 180 μl of Quanti-blue solution (Invivogen, Toulouse, France; rep-qbs) in a flat-bottomed 96-well plate and incubating at 37°C for 2 h. The optical density at 620 nm was measured using a Multiskan plate reader (Fisher Scientific UK Ltd., Loughborough, UK).

Antibodies

Antibodies used in this study were: anti-human CD34 allophycocyanin (APC) conjugated (R&D Systems; FAB7227A – distributed by Bio-Techne Ltd., Abingdon, UK), anti-CD22 phycoerythrin (PE) conjugated (Biolegend UK Ltd, London, UK; 302506) and anti-HA phycoerythrin-cyanine7 (PE-Cy7) conjugated (Biolegend; 901528). All antibodies were diluted 1:50 in phosphate-buffered saline (Gibco; 14190144).

Cell staining & flow cytometry

Cells were harvested for flow cytometry using trypsin/EDTA (Life Technologies; 25200056 – distributed by Fisher Scientific UK Ltd., Loughborough, UK) and stained with antibodies at ambient temperature for 10 min before washing the cells once with phosphate-buffered saline and resuspending in Sytox Blue cell viability dye (Life Technologies; S34857). Stained cells were analyzed by flow cytometry using a MACSQuant 10 flow cytometer (Miltenyi Biotec Ltd., Woking, UK) and downstream analyses were carried out using FlowJo software (FlowJo, OR, USA) . For fluorescence intensity measurements, a gate was drawn around the transfected cell population (Figure 2) or a narrow gate was applied at 10^4 on the marker gene (Figure 3) and the median fluorescence intensity calculated.

$GD2^+$ B16.F10 melanoma immunocompetent mouse model

Splenocytes from C57Bl/6 mice were harvested, stimulated with 2 μg/ml concanavalin A (Sigma Aldrich; C5275-5MG) and 1 ng/ml murine IL-7 (PeproTech EC Ltd., London, UK; 217–17) and transduced with γ-retrovirus pseudotyped with Eco glycoprotein. The cells were cultured for up to 4 days in the presence of 50 U/ml human IL-2 (GenScript Biotech UK Ltd., Oxford, UK; 200368). Cohorts of ten C57Bl/6 mice (Charles River Laboratories, Harlow, UK) were injected subcutaneously with 1×10^5 B16.F10 melanoma cells transduced with a γ-retroviral vector encoding the enzymes GD2- and GD3-synthases to synthesize the ganglioside GD2 and allowed to engraft

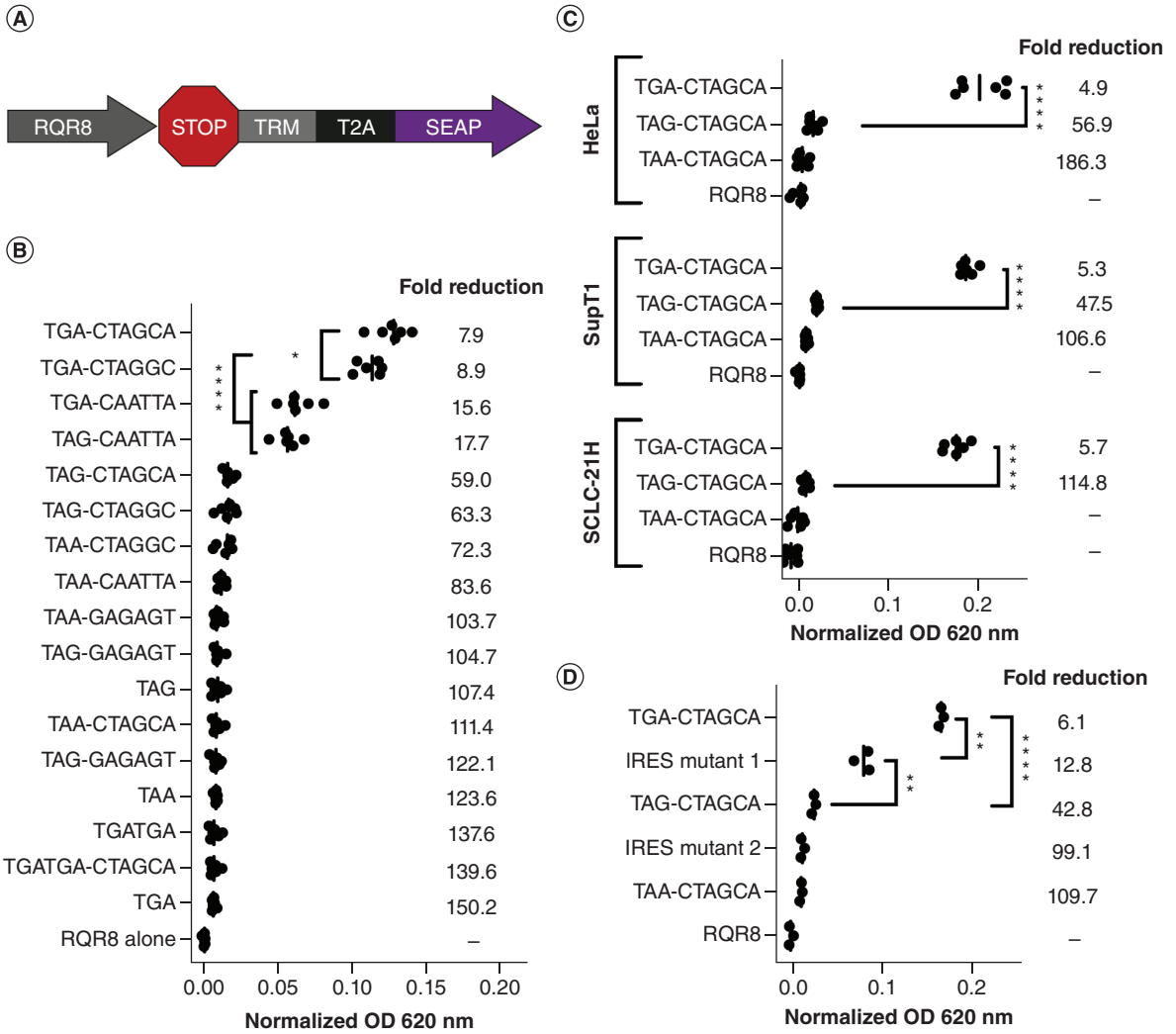

Figure 1. Determination of translational readthrough activity using secreted embryonic alkaline phosphatase. (A) Diagram illustrating the constructs generated to determine translational readthrough motif activity. A stop codon and translational readthrough motif were placed at the 3′ end of the RQR8 sort-select marker coding sequence, 5′ to the SEAP open reading frame. **(B)** SEAP activity was measured in supernatants harvested from 293T cells transfected with the TRM constructs and the data were normalized to the appropriate no-stop (TGG) control. The introduction of a stop codon and TRM reduced SEAP expression between 7.9-fold (TGA-CTAGCA) and 111.4-fold (TAA-CTAGCA) depending on the stop codon used, with TGA being the leakiest codon and TAG and TAA being more stringent. Data represent duplicates from three independent experiments. **(C)** TRMs are functional in HeLa (ovarian adenocarcinoma), SupT1 (T-cell lymphoma) and SCLC-21H (small-cell lung carcinoma) cell lines transduced with the SEAP. Data represent triplicates from two independent experiments. **(D)** Comparison of SEAP expression from TRMs and attenuated encephalomyocarditis virus IRESs in transfected 293T cells showed that a combination of the more stringent stop codons TAG and TAA and TRMs yielded similar expression levels to those obtained using attenuated IRESs. Data represent triplicates from a single experiment. In A–C, mean is shown; statistical analysis was carried out using an unpaired *t*-test with Welch's correction.
*$p < 0.05$; **$p < 0.01$; ****$p < 0.0001$.
IRES: Internal ribosome entry site; SEAP: Secreted embryonic alkaline phosphatase; TRM: Translational readthrough motif.

for 6 days before subjecting the mice to 5 Gy total body irradiation. The following day, mice were intravenously injected with 3×10^6 non-transduced T cells or CAR T cells, and tumor growth and cytokine release monitored for up to 22 days after tumor cell engraftment.

Cytokine secretion

Blood was collected, via tail vein bleed, in heparin-coated tubes (Sarstedt, Nümbrecht, Germany), spun at 2000 × g for 10 min at 4°C and stored at -80°C. Secreted cytokine levels in blood collected from C57Bl/6 mice were measured using a custom Luminex cytokine bead assay (R&D Systems). For murine *in vitro* experiments (presented in Supplementary Figure 1), IL-12 was detected using the murine IL-12

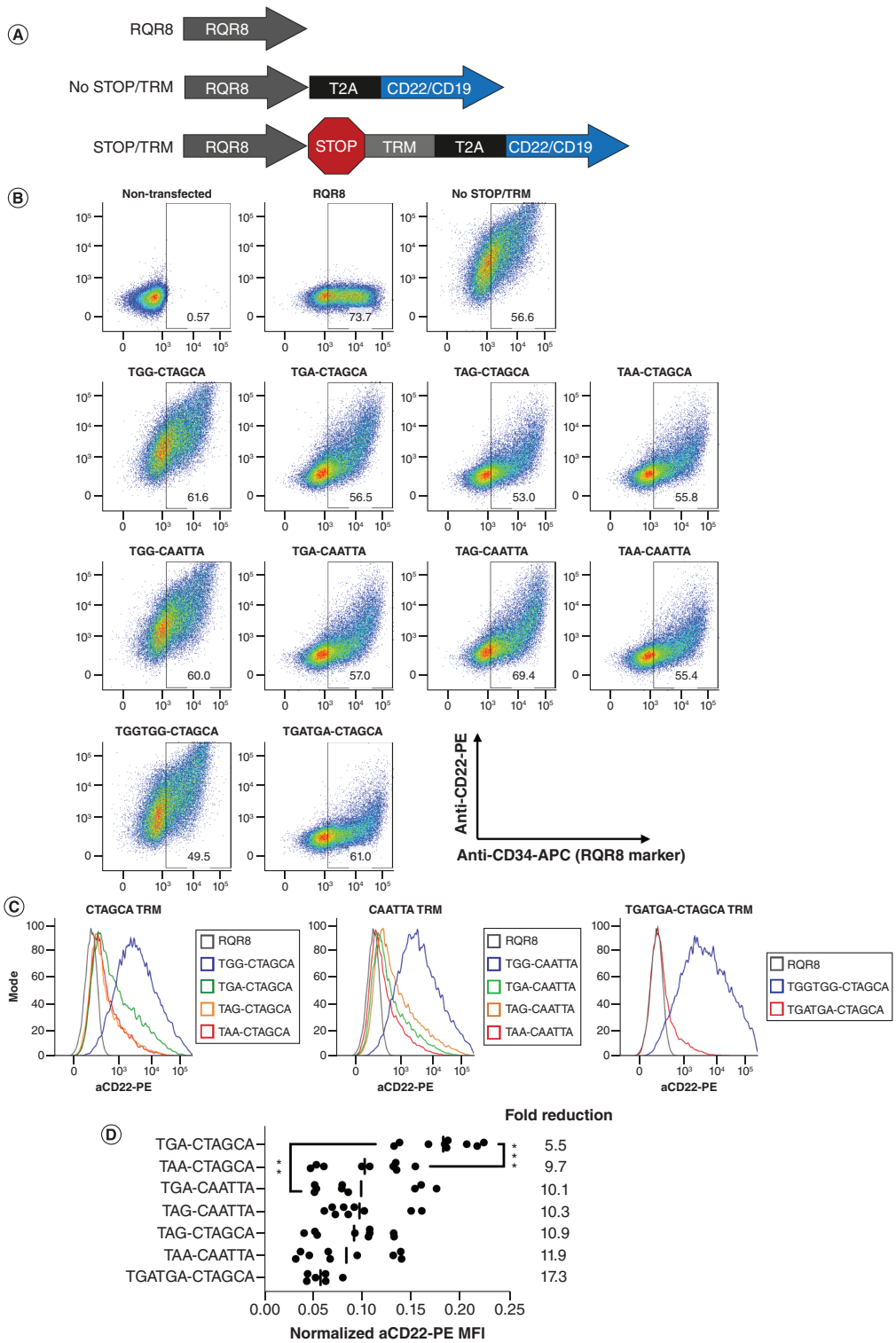

Figure 2. Translational readthrough motifs enable differential expression of transmembrane proteins. (A) A chimera of the ectodomain of human CD22 and the transmembrane and truncated cytoplasmic domain of human CD19 was cloned 3′ to RQR8, a stop codon, a TRM and a self-cleaving peptide sequence. **(B)** Transfected 293T cells were stained with antibodies to anti-CD34 (recognizing the Q-epitope in RQR8) and anti-CD22, and analyzed by flow cytometry. **(C)** Histograms of anti-CD22-PE fluorescence intensity of transfected (RQR8+ cells). The TGA stop codon is the leakiest and permits the highest level of translational readthrough when coupled with the CTAGCA TRM. **(D)** Normalized anti-CD22-PE median fluorescence intensity and fold reduction. Data represent triplicates from three independent experiments. Mean is shown, and statistical analysis was carried using an unpaired *t*-test with Welch's correction: **$p < 0.01$; ***$p = 0.003$.

PE: Phycoerythrin; TRM: Translational readthrough motif.

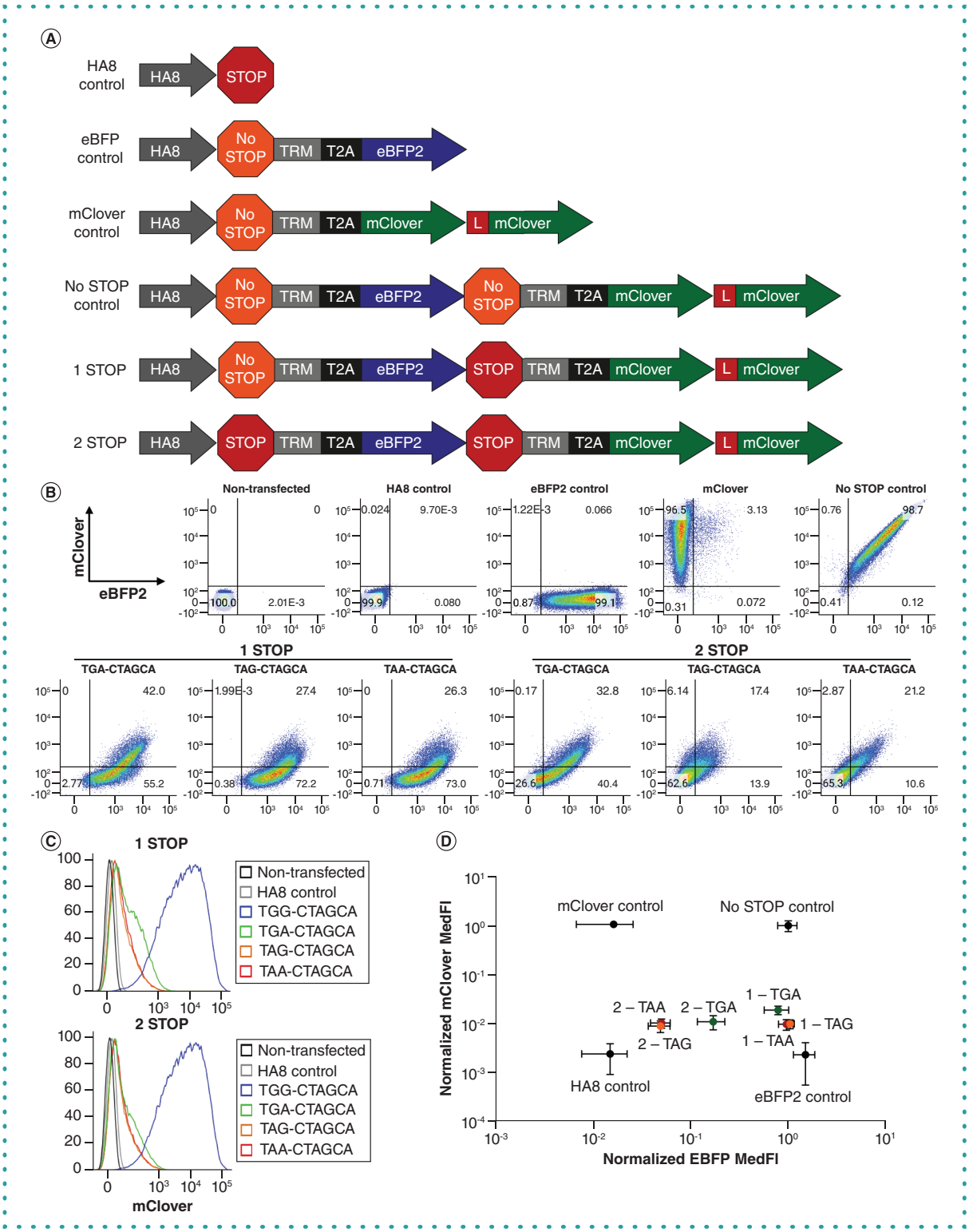

Figure 3. Compound translational readthrough motifs enable fine tuning of transgene expression. **(A)** The fluorescent proteins eBFP2 and tandem mClover were cloned downstream of the cell surface marker HA8 (hemagglutinin epitope presented on a human CD8α stalk). Stop codons, TRMs and self-cleaving peptide sequences were introduced to place either a single stop and TRM or two before the tandem mClover sequence to enable assessment of the impact of placing TRMs in a series on transgene expression. **(B)** Flow cytometry plots of transfected 293T cells. **(C)** Histograms showing tandem mClover fluorescence intensity. A decrease in mClover MedFI is observed when two TGA-CTAGCA motifs are placed in series. **(D)** Quantification of eBFP2 and tandem mClover MedFIs showing that it is possible to fine-tune transgene levels. Data were normalized to the TGG-CTAGCA no-stop control and show the mean and standard deviation of duplicate transfections from three independent experiments. MedFI: Median fluorescence intensity; TRM: Translational readthrough motif.

(p70) ELISA kit (Biolegend; 433604) and IFN-γ using the murine IFN-γ ELISA Kit (Biolegend; 430804). Human IL-12 was detected using the IL-12 p70 Human ELISA Kit, High Sensitivity (ThermoFisher Scientific; BMS238HS).

Statistical analysis

Data were analyzed in GraphPad Prism (Windows 64-bit, version 9.2.0; GraphPad, CA, USA) [30] using an unpaired *t*-test with Welch's correction or ordinary one-way analysis of variance with multiple comparisons.

Results & discussion

Determination of translational readthrough activity using a SEAP reporter system

We began investigating translational readthrough as a means of facilitating differential transgene expression by establishing a SEAP assay. Constructs were cloned where the SEAP sequence was inserted 3′ to the sort-select marker gene RQR8 [25], with an intervening stop codon, TRM and self-cleaving peptide sequence (Figure 1A). TRMs derived from the opioid receptor (OPRL1) [18] (CTAGGC) and tobacco mosaic virus (TMV) [31] (CAATTA) were selected for assessment as these TRMs are known to be functional, along with a modified OPRL1 sequence (CTAGCA) that we predicted to be a functional TRM. The length of the *cis*-acting TRM was limited to six bases to reduce transcriptional burden and minimize the introduction of foreign sequences to the retroviral genome constructs. As controls, constructs lacking TRMs were cloned along with a construct containing the first six bases (GAGAGT) 3′ to the TAG stop codon in feline leukemia virus (FeLV). This hexanucleotide sequence is predicted to be a non-functional TRM by itself, as suppression of the TAG stop codon in FeLV is dependent on an RNA pseudoknot located 3′ to the stop codon [14].

The SEAP constructs were transfected into 293T cells, and downstream analyses carried out 48 h later. The activity of the TRMs was assessed by carrying out SEAP assays on collected supernatant, while the transfection efficiency was determined by staining the cells with anti-CD34 antibody to detect RQR8 and analyzing them by flow cytometry (Figure 1B & data not shown). Quantification of SEAP activity and normalization of the data to the appropriate no-stop (TGG) control demonstrated that the OPRL1 and TMV TRMs were functional, leading to decreased expression ranging from 7.9-fold (TGA-CTGACA motif) to 111.4-fold (TAA-CTAGCA) lower than the no-stop controls (Figure 1B). The lowest level of translational readthrough from the TAA-CTAGCA TRM was comparable to that of the no-TRM controls (TGA 150.2-fold, TAG 107.4-fold and TAA 123.6-fold decrease). In agreement with previously published results, the TGA stop codon was observed to be the leakiest, while the TAG and TAA codons were more stringent in nearly all cases [13,17,18,31]. A notable exception was the TAG-CAATTA TRM, which yielded a similar level of translational readthrough to the TGA equivalent (TGA-CAATTA 15.6-fold and TAG-CAATTA 17.7-fold decrease in SEAP activity). As the TAG stop codon is present in TMV, this result suggests that the CAATTA TRM may have evolved to promote a higher level of translational readthrough. The TRM derived from FeLV was, as predicted, found to be non-functional and promoted background levels of translational readthrough comparable to those of the no-TRM controls (Figure 1B). To investigate whether the use of two stop codons would reduce the level of translational readthrough further than a single stop codon, a construct containing two TGA stop codons and the CTAGCA TRM was generated, along with its equivalent no-stop control. SEAP assays showed that the level of translational readthrough from this motif was 139.6-fold lower than its no-stop control (Figure 1B), indicating that it provided increased termination stringency compared with a single stop and TRM.

The above results indicated that the TRMs were functional in 293T epithelial cells. To investigate whether they were functional in different cell types, SCLC-21H (small-cell lung carcinoma), SupT1 (T-cell lymphoma) and HeLa (ovarian/cervical adenocarcinoma) cells were transduced with the SEAP TRM constructs, and the activity of the secreted enzyme determined (Figure 1C). Similar reductions in SEAP expression were observed as in 293T cells except in the case of SCLC-21H cells, where the TAA-CTAGCA TRM produced barely detectable SEAP expression (Figure 1C). However, the TGA and TAG-CTAGCA TRMs were functional in SCLC-21H cells and, overall, the activity of the TRMs and the hierarchy of stop codon stringency was comparable between the cell lines. Together, these results indicated that TRMs are functional in different cell types and can be used to modulate transgene expression.

Attenuated mutant IRESs have been used to regulate transgene expression [27]. To compare the activity of attenuated IRESs with that of TRMs, we cloned two IRESs derived from the encephalomyocarditis virus IRES upstream of SEAP and determined their activity in transfected 293T cells (Figure 1D). The first mutant IRES, IRES mutant 1, contained an additional A in the JK bifurcation loop [26], while the second mutant, IRES mutant 2, bore the same insertion and six additional mutations (see Materials & methods). Assessment of SEAP activity from transfected 293T cells indicated that IRES mutant 1 reduced expression 12.8-fold, while IRES mutant 2 exhibited a 99.1-fold reduction in SEAP expression (Figure 1D). Our previous data showed that it is possible to achieve similar reductions in transgene expression using TRMs (Figure 1B).

Together, these results demonstrated that TRMs can be exploited to facilitate differential transgene expression and, depending on the TRM utilized, can provide a reduction in expression ranging from 7.9-fold to 139.6-fold lower than multicistronic cassettes lacking a stop codon.

TRMs enable differential expression of transmembrane proteins

CARs are usually directed to tumor-associated antigens that are expressed on the surface of cancer cells [1,2]. Antigen density on the surface of tumors can vary between patients [32], and it is desirable to develop CARs capable of recognizing ultra-low levels of target antigen (<200 copies/cell) to improve the efficacy of CAR-T [33–35]. We hypothesized that TRMs could be employed to develop target

cell lines expressing low levels of antigen, to facilitate the design or identification of CARs sensitive to low levels of tumor antigen. To test this, we generated TRM constructs consisting of the ectodomain of human CD22 fused to the transmembrane and truncated cytoplasmic domain of human CD19, which was cloned downstream of RQR8, a stop codon, a TRM and a self-cleaving peptide sequence (Figure 2A). The constructs were transfected into 293T cells, which were stained 48 h later with anti-CD34 and anti-CD22 antibodies and analyzed by flow cytometry (Figure 2B & C). Quantification and normalization of anti-CD22-PE fluorescence to that of the RQR8 sort-select marker indicated that the TRMs reduced the median fluorescence intensity by 5.5-fold to 17.3-fold, depending on the TRM used (Figure 2D). Consistent with the results obtained from the SEAP assays, the highest level of translational readthrough was observed with the TGA-CTAGCA stop codon and TRM, which reduced CD22 median fluorescence intensity (MedFI) 5.5-fold compared with the no-stop control (Figure 2D). Moreover, when the more stringent TAG and TAA stop codons were used in conjunction with the CTAGCA TRM, CD22 MedFI was reduced 10.9-fold and 9.7-fold, respectively. The level of translational readthrough observed from the CAATAA TRM was similar, with the TGA, TAG and TAA stop codons reducing CD22 MedFI 10.1-fold, 10.3-fold and 11.9-fold, respectively (Figure 2D). The TGATGA-CTAGCA double stop and TRM reduced CD22 MedFI even further, to 17.3-fold less than its no-stop control, demonstrating that the double stop and TRM offered increased termination stringency and lower expression levels.

These data indicated that TRMs can be used to regulate the expression of transmembrane proteins and that it is possible to engineer cell lines expressing a range of target antigen densities for use in cytotoxicity assays to assist with the identification and development of high-sensitivity CARs.

Compound TRMs fine-tune transgene expression

To investigate whether placing two TRMs in a series could be used to compound reductions in transgene expression, constructs were generated in which eBFP2 and two copies of mClover fluorescent protein fused by a linker (tandem mClover) were cloned downstream of the cell surface marker HA8 (Figure 3A). Stop codons and the CTAGCA TRM were introduced upstream of the fluorescent protein coding sequences to generate constructs with either a single stop and TRM before tandem mClover or two. 293T cells were transfected with the constructs and were stained 48 h later with anti-HA antibody and analyzed by flow cytometry (Figure 3B & C). Quantification of anti-HA, eBFP2 and mClover fluorescence intensities indicated that a single stop and TRM placed upstream of mClover reduced MedFI by 52.6-fold with the TGA stop codon and 100.0-fold with both the TAG and TAA stop codons, compared with the no-stop control (Figure 3D). When placed in series, the TGA-CTAGCA stop codon and TRM reduced mClover MedFI 90.9-fold compared with the no-stop control, demonstrating that it is possible to fine-tune transgene expression levels. Interestingly, the addition of a second TAA or TAG stop codon and TRM had no or only a marginal impact on mClover MedFI, with 100.0-fold and 111.1-fold reductions, respectively, compared with the no-stop control. The advantage of using two stop codons and TRMs in tandem is that is possible to achieve a range of transgene expression; accordingly, eBFP2 MedFI was reduced 5.8-fold, 20.4-fold and 20.0-fold with the TGA, TAG and TAA stop codons, respectively, in the constructs containing stop codons and TRMs in series (Figure 3D).

Together, these data show that the TGA-CTAGCA stop codon and TRM are potentially useful for achieving a range of transgene expression levels. Such an approach could be relevant to the purification of multi-subunit complexes where a defined stoichiometry is required.

TRMs enable therapeutically beneficial control of IL-12 secretion

The above data indicated that TRMs could be used to facilitate differential transgene expression, and we next sought to demonstrate their utility in a clinically relevant model. IL-12 is a potent cytokine with therapeutic potential for the treatment of cancer, as it activates macrophages, cytotoxic T cells and natural killer cells, and leads to an enhanced immune response [36]. However, clinical studies have shown that its intravenous administration can result in severe toxicity [37,38], highlighting the need to develop strategies to regulate its expression. To date, approaches to control IL-12 administration include local delivery at the tumor site [39], inducible promoters [40], T cell activation-induced promoters [6,7,41], attenuated internal ribosome entry sites [8,27] and transient mRNA expression [42]. We decided to compare the use of the TGA-CAATTA TRM with the T2A self-cleaving peptide sequence to control the secretion of murine flexi-IL-12, consisting of the p35 and p40 subunits fused together via a flexible linker, in an aggressive immunocompetent mouse model of $GD2^+$ B16.F10 melanoma, to evaluate both efficacy and toxicity. Cohorts of mice were injected with B16.F10 cells transduced with GD2 and GD3 synthases to express the ganglioside GD2 on their cell surface and allowed to engraft for 6 days. The mice were subjected to 5 Gy total body irradiation, to promote CAR T-cell engraftment, and intravenously injected the following day with a 3×10^6 dose of anti-GD2, anti-GD2-T2A-IL-12, anti-GD2-TGA-CAATTA-IL-12 or anti-EGFRvIII-TGA-CAATTA-IL-12 CAR T cells (Figure 4A). All CARs had identical murine CD8α spacer and transmembrane, and CD28 and CD3ζ signaling endodomains. The anti-EGFRvIII CAR was a negative control included in the study to enable the assessment of the effects of IL-12 secretion in the absence of target recognition. The CAR dose was adjusted based on expression of the marker gene Thy1.1.

Tumor volumes were measured for 2 weeks after the injection of CAR T cells (Figure 4B). Mice injected with non-transduced T cells or the control anti-EGFRvIII-TGA-CAATTA-IL-12 CAR failed to control growth of the $GD2^+$ melanoma cells, and only limited control was observed in the cohort injected with the anti-GD2 CAR alone. Robust tumor control was observed in the anti-GD2-T2A-IL-12 and anti-GD2-TGA-CAATTA-IL-12 cohorts; however, mice in the anti-GD2-T2A-IL-12 cohort exhibited dramatic weight loss associated with the

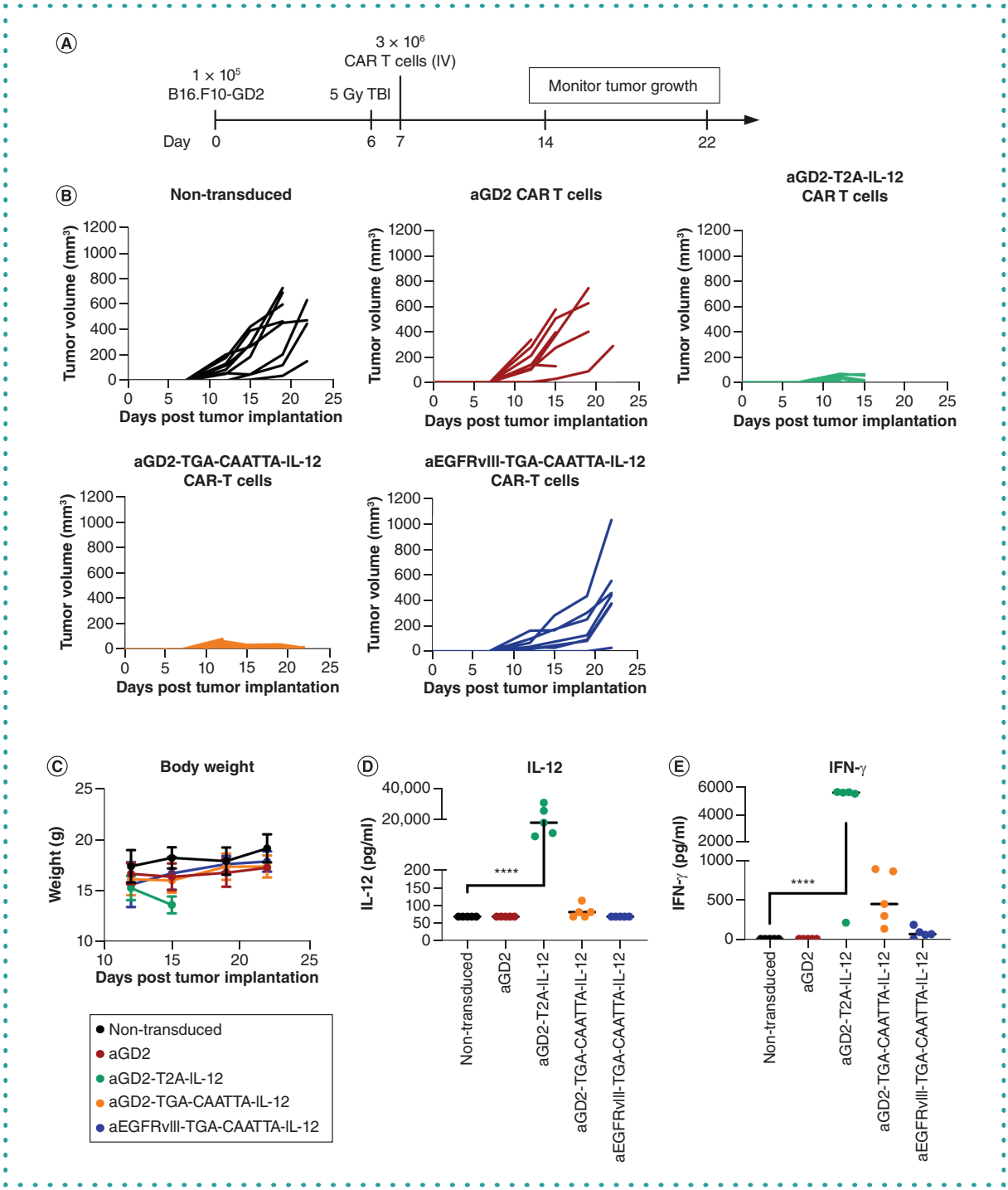

Figure 4. Translational readthrough motifs facilitate therapeutically beneficial levels of IL-12 secretion in an aggressive immunocompetent melanoma mouse model. (A) Timeline of tumor and CAR T-cell engraftment in C57Bl/6 immunocompetent mice. Cohorts of ten mice were subcutaneously injected with 1×10^5 GD2-expressing B16.F10 cells, which were allowed to engraft for 6 days prior to total body irradiation on day 7. A 3×10^6 dose of non-transduced T cells or CAR T cells was intravenously injected via the tail vein, and tumor volume and cytokine secretion were monitored. **(B)** Tumor volume measurements. Mice injected with anti-GD2 CAR T cells expressing IL-12 from a T2A self-cleaving peptide sequence (aGD2-T2A-IL-12 CAR-T) were culled on day 8 post CAR T injection because of cytokine-related toxicity. **(C)** Body weight measurements. The aGD2-T2A-IL-12 CAR-T group rapidly lost body weight and were culled early, while the other groups maintained or increased body weight. **(D & E)** Secreted IL-12 and IFN-γ measurements on day 6 post-CAR T-cell injection. High serum levels of IL-12 and IFN-γ were observed in mice injected with the aGD2-T2A-IL-12 CAR T cells, while considerably lower levels of cytokine secretion were observed from the aGD2-TGA-CAATAA-IL-12 CAR T cells. Importantly, serum IFN-γ levels in the aGD2-TGA-CAATAA-IL-12 CAR T-cell cohort of mice were approximately 8.5-fold lower than those of the aGD2-T2A-IL-12 CAR T-cell group, but higher than those of the aEGFRvIII-TAGA-CAATTA CAR T-cell group, indicating that T-cell activation and IL-12 stimulation led to increased IFN-γ secretion. Data analyzed using ordinary one-way analysis of variance with multiple comparisons.
****$p < 0.0001$.

overexpression of IL-12 and were culled 8 days post CAR T-cell injection (Figure 4C). In contrast, little to no weight loss was observed in the anti-GD2-TGA-CAATTA-IL-12 cohort, indicating that the TRM reduced IL-12 expression, resulting in lower levels of toxicity.

Serum IL-12 and IFN-γ levels were measured in all cohorts 6 days post CAR T-cell injection (Figure 4D & E). The anti-GD2-T2A-IL-12 cohort possessed high levels of IL-12 (mean 19,328 pg/ml ± 9068) and IFN-γ (mean 4528 pg/ml ± 2409), while the anti-GD2-TGA-CAATTA-IL-12 cohort had considerably lower levels of IL-12 (mean 84 pg/ml ± 18) and IFN-γ (mean 531.2 pg/ml ± 333). IL-12 levels in the anti-EGFRvIII-TGA-CAATTA-IL-12 cohort were comparable to those of non-transduced T cells or anti-GD2 CAR alone T cells, indicating that in the absence of T-cell activation, IL-12 secretion remained at background levels. Similarly, no induction of IFN-γ secretion was observed in the anti-EGFRvIII-TGA-CAATTA-IL-12 cohort, whereas IFN-γ levels rose in the serum of mice injected with anti-GD2-TGA-CAATTA-IL-12 CAR T cells, indicating that sufficient IL-12 was being produced to induce IFN-γ secretion. While secreted IL-12 could not be detected from splenocytes transduced with retrovirus expressing IL-12 under the control of a TRM (TGA-CAATTA-IL-12), stimulation of naive splenocytes with conditioned medium from these cells resulted in detectable IFN-γ secretion, albeit at reduced levels compared with the no-TRM (T2A-IL-12) control (Supplementary Figure 1A & B). This suggests IL-12 release below the limit of detection. Furthermore, secreted IL-12 could be detected, by ultrasensitive ELISA, in the medium of human peripheral blood mononuclear cells transduced with retrovirus expressing IL-12 under the control of the same TGA-CAATTA TRM (Supplementary Figure 1C).

Together, the above results are consistent with previously published data showing that IL-12 secretion leads to enhanced tumor clearance in the B16 melanoma mouse model due to reprogramming of myeloid-derived cells in the tumor microenviroment and the induction of an inflammatory response [43]. Exposure of myeloid-derived suppressor cells, macrophages and dendritic cells in the tumor microenvironment results in their reprogramming and activation, which is partly mediated through IFN-γ, leading to antigen cross-presentation and the activation of $CD8^+$ cells that mediate tumor clearance [43]. Our data demonstrate that TRMs can be used to control the expression of potent cytokines and deliver them at levels offering therapeutic benefit for cell-based cancer immunotherapies.

Conclusion

In this paper we have demonstrated that translational readthrough can be harnessed to control transgene expression and have provided examples of how this can be used to identify sensitive CARs responding to low-antigen-density target cells and potentially in a clinical setting to control the expression of the highly potent cytokine IL-12. While the examples given here relate to the CAR T-cell field, we envisage that TRMs will be beneficial to gene- and cell-based therapies, because they are considerably shorter than other regulatory sequences, such as promoters and IRESs, and will save valuable packaging space in vectors. This is particularly pertinent to AAV, which is a vector being more widely adopted for gene- and cell-based therapies [11,12] and has a limited packaging capacity of approximately 5 kb [10].

Translational readthrough is a phenomenon reported to occur on endogenous and viral mRNAs. The background level of translational readthrough is in the order 0.1% [22]; however, translational termination is influenced by sequences flanking the stop codon, with the first six downstream nucleotides being particularly important [22,31,44]. Work carried out on the alphavirus Sindbis, which possesses an in-frame TGA stop codon located between non-structural proteins 3 and 4, showed that the CTA sequence immediately 3′ of the TGA stop was important in mediating translational readthrough. Furthermore, mutation of the cytidine within this sequence to any other nucleotide decreased translational readthrough efficiency from 10 to 1% in a rabbit reticulocyte *in vitro* transcription and translation system [22]. Analysis of 91 viral RNAs identified six triplet sequences immediately downstream of the stop codon that were highly represented and accounted for 90% of the 64 possible combinations, indicating a strong bias toward these sequences for promoting translational readthrough. Again, the sequence CTA was one of the six viral sequences identified, and a longer variant of this motif (CTAG) is also found in endogenous mRNAs, including those of the opioid receptors *OPRK1* and *OPRL1*, *MAPK10* and *AQP4* [18]. Given that the CTAG is known to promote translational readthrough [18], and there is evidence indicating that an adenine at the last position of the hexanucleotide sequence is important [44], we devised the sequence CTAGCA for testing as a TRM. The data presented here demonstrate that the CTAGCA is a functional TRM and suppresses translational termination to a similar extent as the previously tested *OPRL1* motif CTAGGC (Figure 1B). It is interesting to note that the TMV TRM promoted a similar level of translational readthrough when coupled with either the leakier TGA stop codon or with the more stringent TAG stop codon – the stop present in TMV [31] – indicating that there are context-dependent effects and possibly suggesting that this TRM evolved to function with the TAG stop codon.

Fine-tuning of TRM activity could be achieved by placing TRMs in series (Figure 3). By assembling TRMs in series, it is possible to construct vectors where transgenes are expressed at increasingly lower levels, which could be useful for the expression of highly potent (cytokines/hormones) or toxic molecules (diphtheria/anthrax lethal toxin). Such an approach could be useful in the development of combination immunotherapies with PD-1 and CTLA-4 immune checkpoint inhibitors, as these are more efficacious than monotherapies, but carry a higher risk of toxicity due to immune-related adverse advents [45,46]. An alternative approach to TRM fine-tuning would be to include a tRNA sequence to promote readthrough. Recent work suggests that overexpression of tryptophan- and tyrosine-encoding tRNAs in the cell [47] can increase the efficiency of translational readthrough.

We have shown that TRMs can be exploited to facilitate differential expression of transgenes and that their use is broadly applicable to enable the defined expression of secreted (Figure 1), transmembrane (Figure 2) and cytosolic (Figure 3) proteins. Furthermore, we have demonstrated in a clinically relevant aggressive melanoma model that TRMs can be harnessed to control the expression of potent cytokines, such as IL-12, leading the way to their adoption in other gene- and cell-based therapies (Figure 4). Achieving the desired level

of transgene expression would require the testing of different TRMs in the applicable system, but the data provided in this paper offer a valuable starting point for the design of such constructs. As translational readthrough is widely reported in metazoa [13,15,18,48], as well as in bacteria [49], yeast [50] and viruses [20–22], TRMs could be exploited to facilitate differential transgene expression in multiple systems and applications. These could include bioengineering processes, such as: the purification of multi-subunit recombinant protein complexes where a defined stoichiometry is required; the development of stable producer lines, where a TRM could be used to downregulate the expression of a resistance gene and bias for the selection of high-expressing producer lines; and assay development where a range of ligand expression is desired. Given their compact size (6 bp) and ease of introduction to expression cassettes, we envisage that TRMs will be widely adopted to control levels of transgene expression, especially in vectors with finite and limited packaging capacity.

Future perspective

The engineering of recombinant DNA vectors will continue to evolve to minimize the size of regulatory elements (promoters, introns and polyadenylation sequences) without compromising their function. This is particularly important when packaging size is limited, such as in AAV, and TRMs represent a compact and simple method for achieving differential transgene expression.

Executive summary

- Achieving regulated gene expression is an important goal in recombinant DNA engineering.
- Current approaches to achieving differential transgene expression rely on the insertion of long regulatory elements (>100 bp) to vectors.
- Translational readthrough is a phenomenon that can be enhanced by translational readthrough motifs (TRMs).
- Inclusion of stop codons and TRMs facilitates differential transgene expression enabling ~sixfold to ~140-fold reduction in expression levels.
- TRMs are short motifs (6 bp) that can be easily inserted to vectors.
- TRMs are ideally suited to viral systems (adeno-associated virus) where packaging size is limited.
- Differential transgene expression by TRMs is functional in viruses, bacteria, yeast and mammalian cells.

Supplementary data

To view the supplementary data that accompany this paper please visit the journal website at: www.future-science.com/doi/suppl/10.2144/btn-2021-0079

Author contributions

J Sillibourne, G Agliardi and M Righi: planning and conception of experiments, experimental work, writing of manuscript; K Smetanova, G Rowley, S Speller, A Dolor, K Lamb, C Allen, R Karattil and F Parekh: generation of reagents, execution of experimental work and data analysis; F Arce Vargas, S Thomas and S Cordoba: planning and conception of experiments; M Pule: planning and conception of experiments, writing of manuscript.

Acknowledgments

The authors would like to thank L Mekkaoui for reading the manuscript and giving critical feedback.

Financial & competing interests disclosure

J Sillibourne, G Agliardi, M Righi, K Smetanova, G Rowley, A Dolor, K Lamb, C Allen, F Parekh, F Arce Vargas, S Thomas, S Cordoba and M Pule are employees of Autolus Therapeutics, plc. The authors hold equity shares or options in Autolus Therapeutics plc. M Pule owns stock in, receives royalty shares from patents licensed to and receives a salary contribution from Autolus Therapeutics, plc. A patent describing the use of translation readthrough motifs to control transgene expression has been filed by Autolus Therapeutics, plc. The authors have no other relevant affiliations or financial involvement with any organization or entity with a financial interest in or financial conflict with the subject matter or materials discussed in the manuscript apart from those disclosed.

No writing assistance was utilized in the production of this manuscript.

Ethical conduct of research

All animal experiments were conducted with the approval of the Autolus ethics committee and the UK Home Office.

References

Papers of special note have been highlighted as: • of interest

1. Pule M, Finney H, Lawson A. Artificial T-cell receptors. *Cytotherapy* 5(3), 211–226 (2003).
2. Sadelain M, Rivière I, Riddell S. Therapeutic T cell engineering. *Nature* 545(7655), 423–431 (2017).
3. Maude SL, Frey N, Shaw PA *et al.* Chimeric antigen receptor T cells for sustained remissions in leukemia. *N. Engl. J. Med.* 371(16), 1507–1517 (2014).
4. Abramson JS, Palomba ML, Gordon LI *et al.* Lisocabtagene maraleucel for patients with relapsed or refractory large B-cell lymphomas (TRANSCEND NHL 001): a multicentre seamless design study. *Lancet* 396(10254), 839–852 (2020).
5. Kochenderfer JN, Dudley ME, Feldman SA *et al.* B-cell depletion and remissions of malignancy along with cytokine-associated toxicity in a clinical trial of anti-CD19 chimeric-antigen-receptor-transduced T cells. *Blood* 119(12), 2709–2720 (2012).
6. Zhang L, Kerkar SP, Yu Z *et al.* Improving adoptive T cell therapy by targeting and controlling IL-12 expression to the tumor environment. *Mol. Ther.* 19(4), 751–759 (2011).
7. Zhang L, Morgan RA, Beane JD *et al.* Tumor-infiltrating lymphocytes genetically engineered with an inducible gene encoding interleukin-12 for the immunotherapy of metastatic melanoma. *Clin. Cancer Res.* 21(10), 2278–2288 (2015).
8. Pegram HJ, Lee JC, Hayman EG *et al.* Tumor-targeted T cells modified to secrete IL-12 eradicate systemic tumors without need for prior conditioning. *Blood* 119(18), 4133–4141 (2012).

• **Describes the use of an IRES to control secretion of IL-12.**

9. Chen YY, Jensen MC, Smolke CD. Genetic control of mammalian T-cell proliferation with synthetic RNA regulatory systems. *Proc. Natl Acad. Sci. USA* 107(19), 8531–8536 (2010).
10. Lee CS, Bishop ES, Zhang R *et al.* Adenovirus-mediated gene delivery: potential applications for gene and cell-based therapies in the new era of personalized medicine. *Genes Dis.* 4(2), 43–63 (2017).
11. Eyquem J, Mansilla-Soto J, Giavridis T *et al.* Targeting a CAR to the TRAC locus with CRISPR/Cas9 enhances tumour rejection. *Nature* 543(7643), 113–117 (2017).
12. Dai X, Park JJ, Du Y *et al.* One-step generation of modular CAR-T cells with AAV–Cpf1. *Nat. Methods* 16(3), 247 (2019).
13. Schueren F, Thoms S. Functional translational readthrough: a systems biology perspective. *PLoS Genet.* 12(8), e1006196 (2016).
14. Beier H. Misreading of termination codons in eukaryotes by natural nonsense suppressor tRNAs. *Nucleic Acids Res.* 29(23), 4767–4782 (2001).
15. Atkins JF, Loughran G, Bhatt PR, Firth AE, Baranov PV. Ribosomal frameshifting and transcriptional slippage: from genetic steganography and cryptography to adventitious use. *Nucleic Acids Res.* 44(15), 7007–7078 (2016).
16. Brown A, Shao S, Murray J, Hegde RS, Ramakrishnan V. Structural basis for stop codon recognition in eukaryotes. *Nature* 524(7566), 493–496 (2015).
17. Tate WP, Cridge AG, Brown CM. 'Stop' in protein synthesis is modulated with exquisite subtlety by an extended RNA translation signal. *Biochem. Soc. Trans.* 46(6), 1615–1625 (2018).
18. Loughran G, Chou M-Y, Ivanov IP *et al.* Evidence of efficient stop codon readthrough in four mammalian genes. *Nucleic Acids Res.* 42(14), 8928–8938 (2014).

• **Identifies translational readthrough motifs in endogenous genes and carries out mutational studies to determine key *cis*-acting sequences 3′ and 5′ of TRMs.**

19. Schueren F, Lingner T, George R *et al.* Peroxisomal lactate dehydrogenase is generated by translational readthrough in mammals. *Elife.* 3, e03640 (2014).
20. Yoshinaka Y, Katoh I, Copeland TD, Oroszlan S. Murine leukemia virus protease is encoded by the *gag-pol* gene and is synthesized through suppression of an amber termination codon. *Proc. Natl Acad. Sci. USA* 82(6), 1618–1622 (1985).
21. Alam SL, Wills NM, Ingram JA, Atkins JF, Gesteland RF. Structural studies of the RNA pseudoknot required for readthrough of the *gag*-termination codon of murine leukemia virus. *J. Mol. Biol.* 288(5), 837–852 (1999).
22. Li G, Rice CM. The signal for translational readthrough of a UGA codon in Sindbis virus RNA involves a single cytidine residue immediately downstream of the termination codon. *J. Virol.* 67(8), 5062–5067 (1993).
23. Wills NM, Gesteland RF, Atkins JF. Evidence that a downstream pseudoknot is required for translational read-through of the Moloney murine leukemia virus *gag* stop codon. *Proc. Natl Acad. Sci. USA* 88(16), 6991–6995 (1991).

• **Identifies an RNA pseudoknot as being important for translational readthrough.**

24. Büeler H, Mulligan RC. Induction of antigen-specific tumor immunity by genetic and cellular vaccines against MAGE: enhanced tumor protection by coexpression of granulocyte-macrophage colony-stimulating factor and B7-1. *Mol. Med.* 2(5), 545–555 (1996).
25. Philip B, Kokalaki E, Mekkaoui L *et al.* A highly compact epitope-based marker/suicide gene for easier and safer T-cell therapy. *Blood* 124(8), 1277–1287 (2014).
26. Bochkov YA, Palmenberg AC. Translational efficiency of EMCV IRES in bicistronic vectors is dependent upon IRES sequence and gene location. *BioTechniques* 41(3), 283–292 (2006).
27. Wijewarnasuriya D, Bebernitz C, Lopez AV, Rafiq S, Brentjens RJ. Excessive costimulation leads to dysfunction of adoptively transferred T cells. *Cancer Immunol. Res.* 8(6), 732–742 (2020).
28. Kuan C-T, Reist CJ, Foulon CF *et al.* 125I-labeled anti-epidermal growth factor receptor-vIII single-chain Fv exhibits specific and high-level targeting of glioma xenografts. *Clin. Cancer Res.* 5(6), 1539–1549 (1999).
29. Nakamura K, Tanaka Y, Shitara K, Hanai N. Construction of humanized anti-ganglioside monoclonal antibodies with potent immune effector functions. *Cancer Immunol. Immunother.* 50(5), 275–284 (2001).
30. Swift ML. GraphPad Prism, data analysis, and scientific graphing. *J. Chem. Inf. Comput. Sci.* 37(2), 411–412 (1997).
31. Cassan M, Rousset J-P. UAG readthrough in mammalian cells: effect of upstream and downstream stop codon contexts reveal different signals. *BMC Mol. Biol.* 2(3), 8 (2001).
32. Fry TJ, Shah NN, Orentas RJ *et al.* CD22-targeted CAR T cells induce remission in B-ALL that is naive or resistant to CD19-targeted CAR immunotherapy. *Nat. Med.* 24(1), 20–28 (2018).
33. Shah NN, Fry TJ. Mechanisms of resistance to CAR T cell therapy. *Nat. Rev. Clin. Oncol.* 16(6), 372 (2019).
34. Walker AJ, Majzner RG, Zhang L *et al.* Tumor antigen and receptor densities regulate efficacy of a chimeric antigen receptor targeting anaplastic lymphoma kinase. *Mol. Ther.* 25(9), 2189–2201 (2017).
35. Majzner RG, Rietberg SP, Sotillo E *et al.* Tuning the antigen density requirement for CAR T-cell activity. *Cancer Discov.* 10(5), 702–723 (2020).
36. Yeku OO, Brentjens RJ. Armored CAR T-cells: utilizing cytokines and pro-inflammatory ligands to enhance CAR T-cell anti-tumour efficacy. *Biochem. Soc. Trans.* 44(2), 412–418 (2016).
37. Lacy MQ, Jacobus S, Blood EA, Kay NE, Rajkumar SV, Greipp PR. Phase II study of interleukin-12 for treatment of plateau phase multiple myeloma (E1A96): a trial of the Eastern Cooperative Oncology Group. *Leuk. Res.* 33(11), 1485–1489 (2009).
38. Leonard JP, Sherman ML, Fisher GL *et al.* Effects of single-dose interleukin-12 exposure on interleukin-12 – associated toxicity and interferon-G production. *Blood* 90(7), 2541–2548 (1997).
39. Agliardi G, Liuzzi AR, Hotblack A *et al.* Intratumoral IL-12 delivery empowers CAR-T cell immunotherapy in a pre-clinical model of glioblastoma. *Nat. Commun.* 12(1), 444 (2021).
40. Alsaieedi A, Holler A, Velica P, Bendle G, Stauss HJ. Safety and efficacy of Tet-regulated IL-12 expression in cancer-specific T cells. *OncoImmunology* 8(3), 1542917 (2019).
41. Chmielewski M, Kopecky C, Hombach AA, Abken H. IL-12 release by engineered T cells expressing chimeric antigen receptors can effectively muster an antigen-independent macrophage response on tumor cells that have shut down tumor antigen expression. *Cancer Res.* 71(17), 5697–5706 (2011).
42. Etxeberria I, Bolaños E, Quetglas JI *et al.* Intratumor adoptive transfer of IL-12 mRNA transiently engineered antitumor CD8+ T cells. *Cancer Cell* 36(6), 613–629.e7 (2019).
43. Kerkar SP, Goldszmid RS, Muranski P *et al.* IL-12 triggers a programmatic change in dysfunctional myeloid-derived cells within mouse tumors. *J. Clin. Invest.* 121(12), 4746–4757 (2011).
44. Harrell L. Predominance of six different hexanucleotide recoding signals 3′ of read-through stop codons. *Nucleic Acids Res.* 30(9), 2011–2017 (2002).
45. Michot JM, Bigenwald C, Champiat S *et al.* Immune-related adverse events with immune checkpoint blockade: a comprehensive review. *Eur. J. Cancer* 54, 139–148 (2016).
46. Hodi FS, O'Day SJ, McDermott DF *et al.* Improved survival with ipilimumab in patients with metastatic melanoma. *N. Engl. J. Med.* 363(8), 711–723 (2010).
47. Beznosková P, Bidou L, Namy O, Valášek LS. Increased expression of tryptophan and tyrosine tRNAs elevates stop codon readthrough of reporter systems in human cell lines. *Nucleic Acids Res.* 49(9), 5202–5215 (2021).
48. Jungreis I, Lin MF, Spokony R *et al.* Evidence of abundant stop codon readthrough in *Drosophila* and other metazoa. *Genome Res.* 21(12), 2096–2113 (2011).
49. Poole ES, Brown CM, Tate WP. The identity of the base following the stop codon determines the efficiency of *in vivo* translational termination in *Escherichia coli*. *EMBO J.* 14(1), 151–158 (1995).
50. Namy O. Identification of stop codon readthrough genes in *Saccharomyces cerevisiae*. *Nucleic Acids Res.* 31(9), 2289–2296 (2003).